ELSEVIER

Journal of Nuclear Materials 296 (2001) 265–272

journal of nuclear materials

www.elsevier.com/locate/jnucmat

Behaviour of F82H mod. stainless steel in lead–bismuth under temperature gradient

D. Gómez Briceño *, F.J. Martín Muñoz, L. Soler Crespo, F. Esteban, C. Torres

CIEMAT, Nuclear Fission Department, Avda. Complutense 22, 28040 Madrid, Spain

Abstract

Austenitic steels can be used in a hybrid system in contact with liquid lead–bismuth eutectic if the region of operating temperatures is not beyond 400°C. For higher temperatures, martensitic steels are recommended. However, at long times, the interaction between the structural material and the eutectic leads to the dissolution of some elements of the steel (Ni, Cr and Fe, mainly) in the liquid metal. In a non-isothermal lead–bismuth loop, the material dissolution takes place at the hot leg of the circuit and, due to the mass transfer, deposition occurs at the cold leg. One of the possible ways to improve the performance of structural materials in lead–bismuth is the creation of an oxide layer. Tests have been performed in a small natural convection loop built of austenitic steel (316L) that has been operating for 3000 h. This loop contains a test area in which several samples of F82Hmod. martensitic steel have been tested at different times. A gas with an oxygen content of 10 ppm was bubbled in the hot area of the circuit during the operation time. The obtained results show that an oxide layer is formed on the samples introduced in the loop at the beginning of the operation and this layer increases with time. However, the samples introduced at different times during the loop operation, are not protected by oxide layers and present material dissolution in some cases.

1. Introduction

Hybrid systems, so-called accelerator driven systems (ADS), are an interesting alternative to the underground disposal of high level radioactive wastes generated in power nuclear reactors. They are designed to transmute long-life and high activity wastes. The neutrons to transform or eliminate the long-life isotopes come from the spallation reaction. A high energy proton beam impacts into a target in which the spallation reaction takes place, producing fission neutrons and thermal energy. The physico-chemical and nuclear characteristics of lead–bismuth eutectic make this heavy liquid metal suitable to be used as spallation target and as coolant in a hybrid system, [1]. However, heavy liquid metals, and particularly lead–bismuth, present a high corrosivity to most of the structural materials.

Austenitic steels may be used in a hybrid system in contact with liquid lead–bismuth if the region of operating temperatures is not beyond 400°C. For higher temperatures, martensitic steels are recommended [2]. However, with long operation times, the interaction between the structural material and the eutectic leads to the dissolution of some elements of the steel (Ni, Cr and Fe, mainly) in the liquid metal [3]. In a non-isothermal lead–bismuth loop, the material dissolution takes place at the hot leg of the circuit and, due to mass transfer, deposition occurs at the cold leg. The available experience, proceeding from the former USSR, shows that one of the possible ways to improve the performance of structural materials in lead–bismuth is the formation and maintenance of a protective oxide layer, which would constitute a barrier between the liquid metal and the steel.

Experimental work has been performed in a thermal convection loop in order to gain some insight into the evolution of the behaviour of martensitic stainless steel

* Corresponding author. Tel.: +34-91 346 6605; fax: +34-91 346 6661.

E-mail address: lola.gomezbriceno@ciemat.es (D. Gómez Briceño).

0022-3115/01/$ - see front matter
PII: S0022-3115(01)00528-1

F82H mod. in lead–bismuth under a temperature gradient in quasi-static conditions.

2. Experimental

Tests have been performed in a small thermal convection loop built of austenitic stainless steel type 316, containing a lead–bismuth volume of 1.2 l. A scheme of the loop is shown in Fig. 1. The loop has a hot leg (550°C) and a cold leg (500–450°C). Thermocouples placed in several points of the loop, embedded in the lead–bismuth, were used to control the loop temperatures. The eutectic and the gas for controlling the atmosphere were introduced into the loop from an expansion tank placed on top of it.

The lead–bismuth was purified by bubbling a reductive gas, argon with 10% H_2, at 400°C during three days in the purification tank. Before the tests a preconditioning of the loop was carried out. The loop was heated at 400°C under vacuum for several hours and, afterwards, argon with 10 ppm of oxygen was flowing through it during 3 h for the prepassivation of the loop. Finally the loop was filled with the eutectic under vacuum. When the loop was completely filled, temperatures were increased up to working temperatures. 24 h after reaching working temperatures, a specimen chain was inserted in the hot zone of the loop.

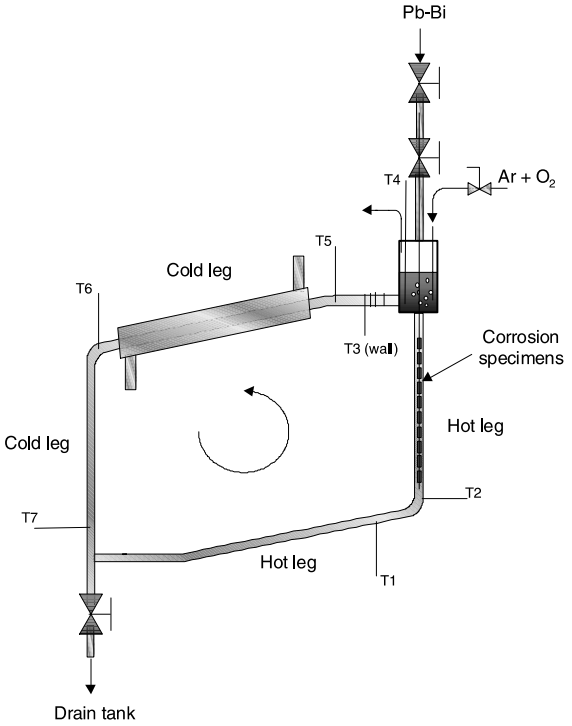

Fig. 1. Thermal convection loop.

Cylindrical specimens (10 mm length and 7 mm diameter) of martensitic steel F82H mod. were tested as well as some specimens of low alloy steel $2^{1/4}$ Cr–Mo. The results of the latter are not described in this paper. The materials composition is shown in Table 1. Specimens were inserted and removed several times from the test zone placed at the hot leg, average temperature ~500°C, during loop operation, without stopping the flowing of lead–bismuth, according to the scheme shown in Fig. 2. During the loop operation, a flow of 40 cm^3/min of argon with 10 ppm of oxygen was bubbled in the hot area of the loop. Oxygen concentration in the melt eutectic was not measured. However an oxygen concentration of 6×10^{-6} wt% was estimated at the beginning of the tests.

After the tests, specimens were examined by optical and scanning electron microscopy. Auger spectroscopy was used to obtain the depth profile compositions of the oxide layers formed on the specimens during the tests. Previously to perform Auger analyses lead–bismuth was

Table 1
Materials composition

Weight%	F82H mod.	$2^{1/4}$ Cr–1Mo
Fe	Bal.	Bal.
Cr	7.750	2.250
Ni	0.015	
Al	0.004	
Mo	0.010	1.000
C	0.100	0.090
Si	0.230	0.200
Ta	0.005	
Ti	0.004	
Mn	0.160	0.450
Nb	<0.01	
S	0.003	<0.015
B	40×10^{-3}	
Co	30×10^{-4}	
Cu	0.030	
V	0.140	<0.030
P	–	<0.015

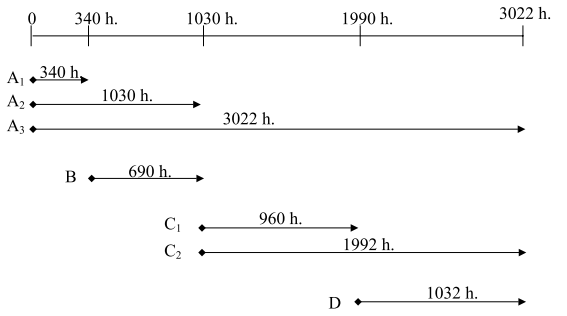

Fig. 2. Test scheme.

mechanically removed from the specimens. The atomic concentrations were calculated according to [4,5] and were normalised to 100%. Sputtering depth profiling was performed using a 3.0 keV argon ion flux, the etching rate calibrations being achieved with a Ta_2O_5 thin film of known thickness.

3. Results

The temperature evolution in different points of the thermal convection loop is represented in Fig. 3. Specimen insertion and removing times are also indicated in this figure. According to the temperature registration, loop operation can be divided into four steps. During all the steps, the thermocouples placed in the hot zone of the loop (T_2, T_4) present uniform values with a light decrease over time. However, the cool zone temperature (T_6, T_7) oscillates during the first step and stabilises at the beginning of the second step. From this level, it decreases 50°C, and it soars to a higher level than the existent at the beginning of the second step. All this process occurs in a time bracket of 1000 h of operation. During the third step, the temperature decreases again, reaching lower minimum values than in the previous case, after 1700 h of operation. During the last step, the temperatures stabilise again until the end of the loop operation, keeping a temperature gradient between the hot and the cool zones of ~80°C. Temperature decreases may be due to slag formation hindering lead–bismuth flowing. However, loop plugging has not been observed. Sudden minimum temperature increases in the cool zones may be due to slag dissolution. A constant flow of gas was kept, during all the operation.

As was mentioned above, in this paper only the results of the F82H mod. will be presented and discussed. The six specimens (type A) incorporated into the loop at the beginning of the operation show a good corrosion resistance. All the samples are covered by an homogeneous oxide layer, with minor spalling areas in samples A_2 and A_3. The type A_1 specimens, tested for 340 h, present a thin oxide layer of 2.5–3.5 μm, formed by two sublayers. The outer layer, of 1–1.5 μm thickness, is iron oxide and the inner layer is formed by iron, chromium and oxygen with a chromium concentration higher than its value in the alloy, as can be seen in the Auger depth profiles, Fig. 4. A slight depletion of chromium in the underlying alloy was detected.

Type A_2 specimens, tested for 1030 h, show an oxide layer very similar in composition and thickness to the ones detected in A_1 specimens, Fig. 5. However, A_3 specimens, tested for 3022 h, from the beginning to the end of the loop operation, present an oxide layer with a thickness of 20 μm but with similar composition to A_1 and A_2 specimens. Fig. 6, shows that in A_3 specimens the outer layer is formed by iron and oxygen, magnetite, whereas the inner layer has iron, chromium and oxygen, with the higher concentration of chromium placed in the interface between the inner layer and the alloy. Auger analysis shows no chromium depletion in the underlying alloy of A_3 specimens contrary to that observed in A_1 specimens. However, in a metallographic cross-section of A_3 specimen, Fig. 7, oxide particles are observed in the underlying alloy as a consequence of an oxidation process. EDX analysis points out that the particle composition corresponds to a spinel. In all A specimens, the outer layer composition corresponds to magnetite whereas inner layer is an $Fe(Fe_{2-x})Cr_xO_4$. Lead–bismuth eutectic (named lead in all the figures) is incorporated to the outer layer in all A specimens.

Type B specimens were introduced into the loop after 340 h of the operation beginning, and removed 690 h later. These specimens present a general dissolution in most of the surface. A polished cross-section of the

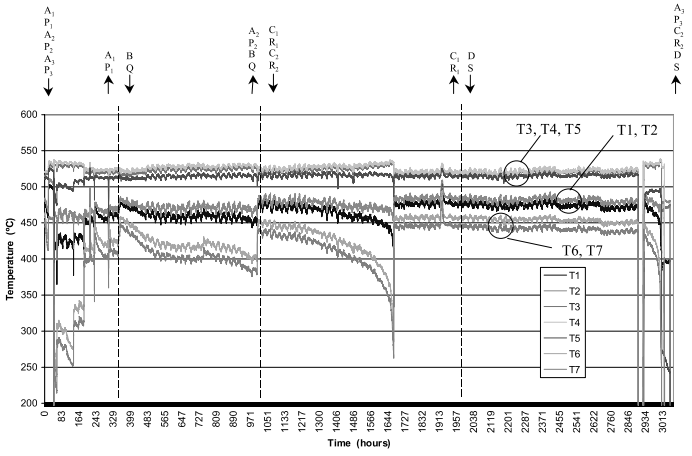

Fig. 3. Temperature evolution during loop life.

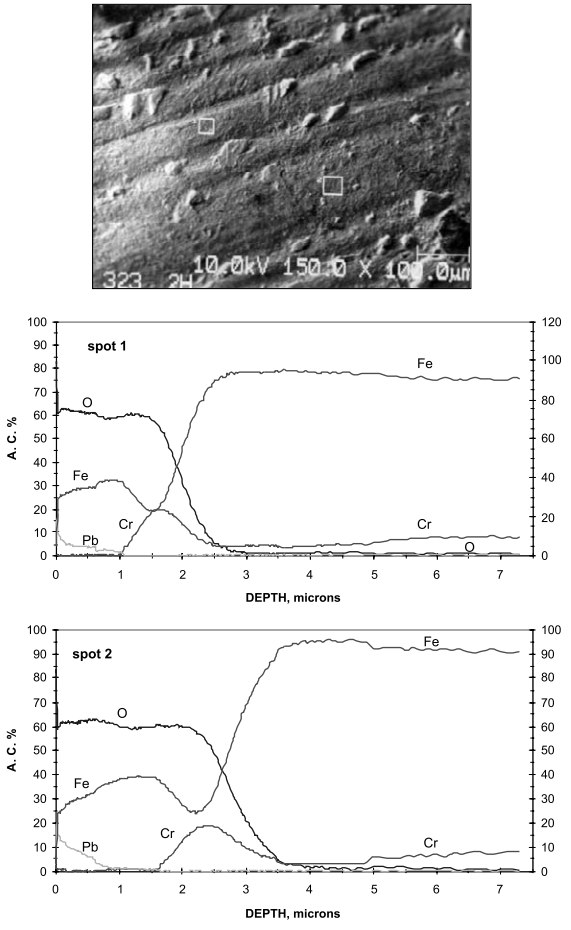

Fig. 4. Auger composition depth profile, A_1 specimen, 340 h.

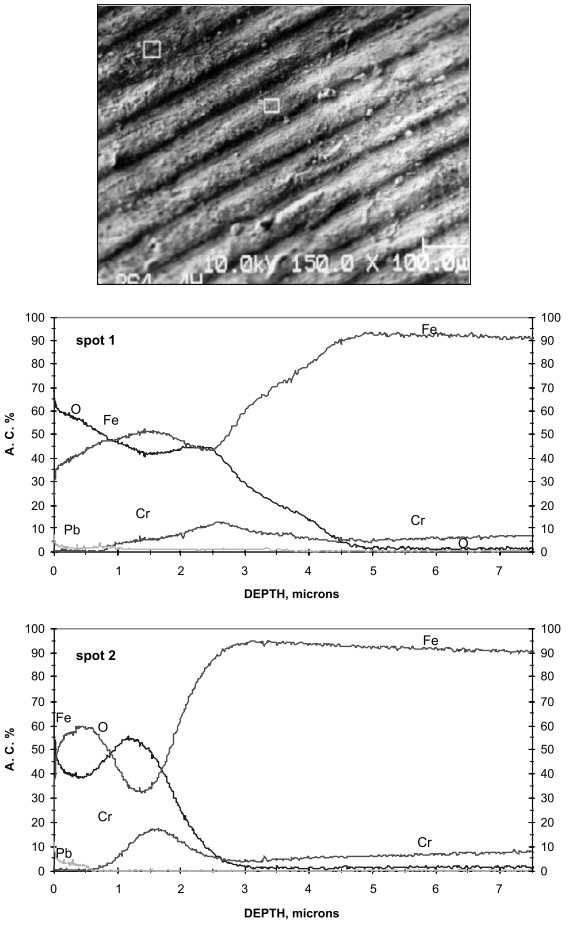

Fig. 5. Auger composition depth profile, A_2 specimen, 1030 h.

sample was used to measure the depth attack, taking unattacked areas as a zero line, Fig. 8. The maximum depth attack in the B specimens is 50 μm. Auger analyses of small unattacked areas covered by a very thin oxide layer show a single oxide layer formed by chromium and oxygen. Type C specimens inserted into the loop after 1030 h of the operation beginning were removed 960 h afterwards (C_1 specimen) and 1992 h afterwards (C_2 specimen). Both specimens show general dissolution with a depth attack up to 140 μm in specimen C_2, measured on a polished cross-section. Small surface areas covered by a thin oxide layer are still visible. A representative dissolution area is shown in photo (a) in Fig. 9 and an area covered by a thin oxide layer in photo (b) in the same figure. In both cases, depth profile composition analyses were performed in two spots of each area with similar results. In the dissolution area, the Auger analyses show no oxygen and chromium depletion, Fig. 9, in contrast with the results obtained in the area covered by a thin oxide layer. In this case, chromium enrichment associated with oxygen was detected, Fig. 9. The thickness and the composition of this oxide layer are similar to the observed in type B specimens.

Type D specimen was introduced into the loop 2000 h after the beginning of the operation and removed at the end of the tests together with A_3 specimen. No dissolution was observed in this sample. Auger analysis shows a single thin layer of less than 1 μm covering the entire specimen, with a high chromium concentration and without iron, Fig. 10. In this sample, lead is incorporated to the oxide layer rich in chromium. After 2000 h from the beginning of the operation a lead–bismuth sample was taken out from the loop in order to measure impurities by ICP–AES. This sample had 265 ppm nickel, 5.4 ppm chromium and 17 ppm iron. Iron concentration is higher than iron solubility in eutectic (3.6 ppm), while nickel and chromium concentration values are lower than their solubility values at 530°C (30212 and 13.8 ppm, respectively), [6].

After the end of the tests, the loop was cut to be destructively examined. Samples of solidified lead–bis-

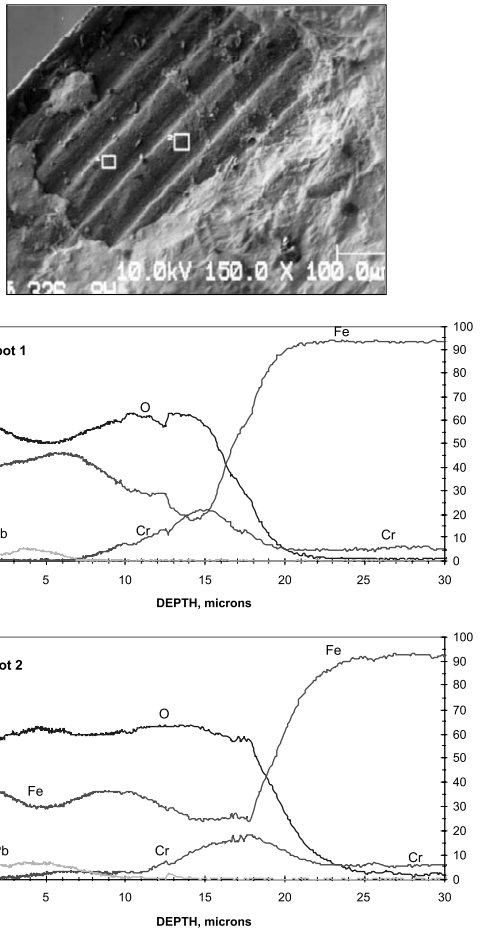

Fig. 6. Auger composition depth profile, A_3 specimen, 3022 h.

muth from the hot and cold zones were taken to measure oxygen by LECO. A heterogeneous oxygen distribution was observed in the samples. At the core, 2 ppm oxygen were observed in the hot zone, and 1 ppm oxygen in the cold zone. Near the walls, 9 ppm oxygen were measured in the hot zone and 6 ppm oxygen in the cold zone.

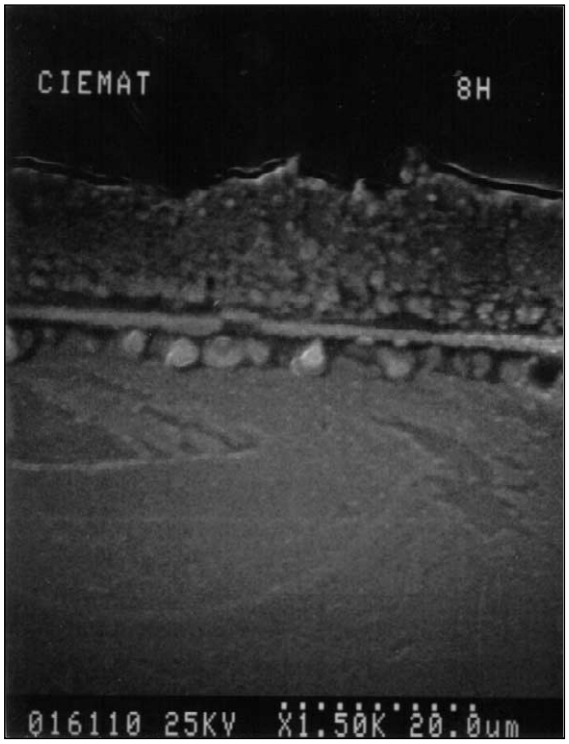

Fig. 7. Metallographic cross-section of A_3 specimen, 3022 h.

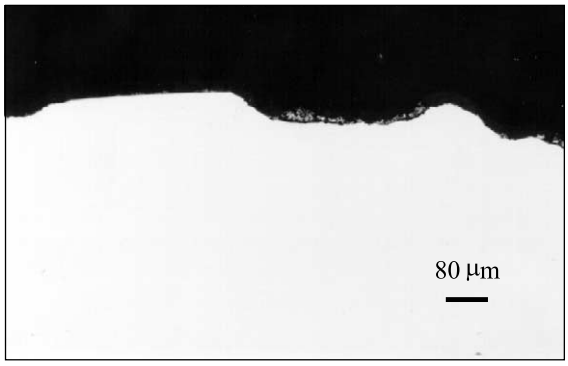

Fig. 8. Metallographic cross-section of B specimen, 690 h.

4. Discussion

Liquid metal corrosion depends on the solution rate and the solubility value of the solid metal in the liquid metal. Lead alloys, and in particular lead–bismuth eutectic, show a higher aggressivity to the structural materials than the alkali liquid metals. In a static system, solution of the solid metal occurs until the solubility value of the main elements of the alloy is reached. In a dynamic system with temperature gradient, a mass transfer process occurs. The dissolved material at the hot zone is deposited at the cold zone, and the elements concentration in the liquid metal represents a steady-state balance between the rates of solution and precipitation in different zones of corroding systems [7].

Oxygen activity in lead and lead alloys has a significant influence on the corrosion/protection of structural materials. For high oxygen activity the corrosion of iron–chromium alloy is higher than for iron whereas for low oxygen activity the alloy presents higher resistance corrosion, [9]. Formation of oxide layer on the structural materials can prevent the alloy solution.

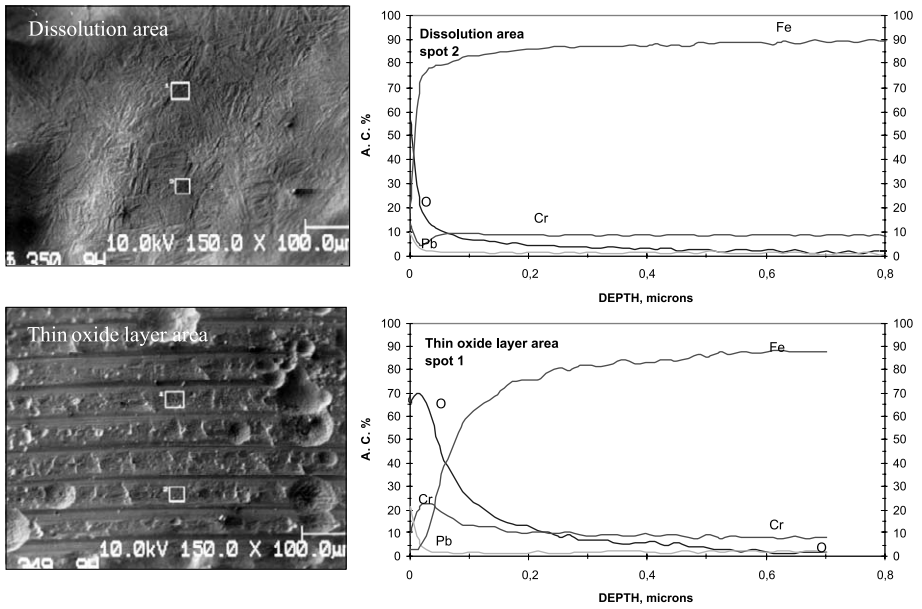

Fig. 9. Auger composition depth profile, C_2 specimen, 1992 h.

A general consideration of the results seems to point out that the oxygen content in the loop is not enough to form oxide layers on the specimens placed in the hot zone of the loop. In fact specimens B and C present material solution and no oxide layers. However, in the type A specimens tested at the same time in the loop, an appreciable growing of the oxide layer was detected. This observation raises some questions about the first consideration.

Type A specimens inserted into the loop at the beginning of the operation are covered by an homogeneous double oxide layer. The thickness of this oxide layer reaches 20 μm after 3022 h. The growth of this oxide layer is almost inappreciable between 340 and 1032 h, and then it grows significantly up to 3022 h. These results seem to be in accordance with the general behaviour accepted for the oxidation of iron–chromium alloys and stainless steel [8] After an initial protective period, a sudden increase in rate occurs once the breakaway time has been reached. This stage is often followed by a further reduction in rate by a self-healing process. This last step has not been observed in our tests, probably due to their short duration. The oxide layers of type A specimens show similar characteristic. The inner oxide layer, $Fe(Fe_{2-x})Cr_xO_4$, seems to be protective enough to prevent lead–bismuth penetration. No eutectic is incorporated to this layer contrary to the observed in iron oxide outer layer. Eutectic concentration in the outer layer decreases and disappears in the interface outer/inner oxide layer.

The information on the oxidation behaviour of stainless steels in liquid lead–bismuth is very scarce. However, it is accepted than the available information on stainless steels oxidation in molten lead can be useful to analyse the materials behaviour in lead–bismuth. Fedirko et al. [9] found that spinel rich in chromium can protect iron–chromium alloys in molten lead. These authors tested Armco iron, Fe–16Cr and Fe–16Cr–1Al in stagnant liquid lead at 600°C, with some amount of lead oxide to get a concentration of 10^{-5} wt% oxygen. After 1000 h of testing, four different zones could be observed on the transverse microsections of Fe–16Cr–1Al. The first zone was a porous oxide layer with a high concentration of iron and lead and a low concentration of chromium and aluminium. This zone was formed by magnetite and lead. Lead concentration decreased with the distance from the surface, but on the interface of the first and the second zone lead was present. The second zone was a continuous oxide film enriched with chromium and aluminium. The composition of this film was an Fe_3O_4–$FeCr_2O_4$ solid solution with the spinel structure. Lead was not present in the interface between the second and third zone. A process of internal oxidation with chromium and aluminium oxides mainly along grain boundaries was detected in the third zone. Finally the fourth zone had the matrix composition but grain boundaries also contained oxide compounds. Contrary to the observation in oxygen saturated melts [10], spinel rich in chromium is not permeable for lead in solutions with low oxygen concentration of 10^{-5} wt% [9].

In addition, in static tests performed in oxygen saturated molten lead at 520°C, Benamati et al. [11] observed the formation of continuous layers of reaction products with an average thickness of 20 μm after 2000 h

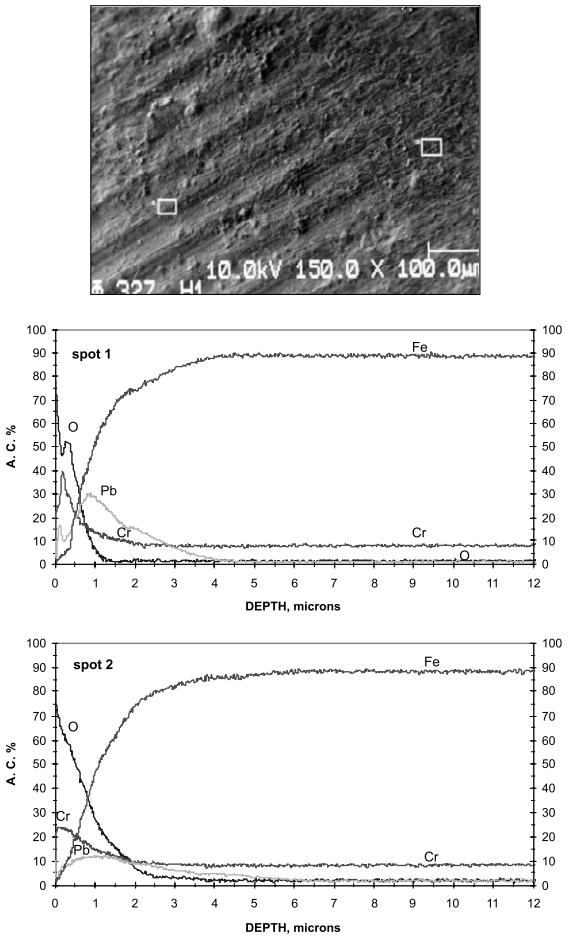

Fig. 10. Auger composition depth profile, D specimen, 1032 h.

and of 40 μm after 3700 h in martensitic steel F82H mod. specimens. The reaction product layers were formed by two distinct sublayers of Me_3O_4. Only the inner one contained chromium in addition to iron. Lead was detected in the outer sublayer of all the product layers. These authors point out that oxide layers formed in oxygen saturated liquid lead containing an additional source of oxygen in the form of lead oxide are not protective against oxidation, since the oxide layer thickness increases along with the exposure time.

On the other hand, Müller et al. [12] found oxide layers of similar characteristics to the observed in the type A specimens in samples of a martensitic steel with 9.99 Cr (Optifer) tested in stagnant liquid lead containing 8×10^6 at.% oxygen, at 550°C, under controlled $Ar–H_2/H_2O$ atmosphere. Muller observed a corrosion attack with three different zones. The outer layer consisted of magnetite without appreciable chromium concentration. A middle layer formed by Cr–Fe spinel, with a chromium concentration lower than the detected in the A_3 specimens, and an internal oxygen diffusion zone in which oxides precipitate along the grain boundaries could be observed. After 3000 h, the thicknesses of magnetite and spinel were 20 and 15 μm, respectively whereas the depth of diffusion zone was 10 μm.

According to Fedirko et al. [9], in liquid lead with low activity of oxygen, the formation of the external oxide layer based on Fe_3O_4 is very low and significant amounts of active alloying elements are accumulated in the more internal layers. The lack of mobility of chromium through the magnetite lattice explains the formation of the spinel layer. Faster diffusing elements like manganese and iron will pass through to the outer layer, while slower diffusing elements like chromium will be oxidised without movement and remain in the inner layer. Both magnetite and spinels M_3O_4 are based on a close-packed cubic sublattice of oxygen ions in which the metals ions are the faster moving species and determine the oxidation rates. Thus, in a martensitic steel, chromium moves more slowly than iron. The outer layer is formed by magnetite and the inner layer consists of iron, chromium spinels. The inner layer grows inward from the original metal surface. The oxygen transport through this layer can take place via pores within the inner layer, since solid state diffusion of oxygen through the magnetite lattice is too low [13]. The Auger analysis results point out that the composition of the outer oxide layer fits well with magnetite composition, and the inner oxide layer corresponds to a spinel $Fe(Fe_{2-x})Cr_xO_4$. Spinel rich in chromium is the typical oxide layer on stainless steels with Cr concentration lower than 13% when they are oxidised at high temperature. Müller et al. [12] consider that no main differences exist between the oxide layers formed in lead and in an oxidation process in a controlled furnace atmosphere at the same temperature.

The thin oxide layer detected on sample D is formed by oxygen and chromium with a minor amount of iron. No chromium depletion was observed in the underlying alloy. In spite of having a high chromium concentration, this layer allows the eutectic penetration, whose concentration has a maximum in the oxide/alloy interface and apparently penetrates in the base alloy underneath the oxide/alloy interface. No external iron oxide has been detected in this sample. The lack of iron external oxide layer can be a consequence of two causes, not necessarily exclusive. On one hand, oxygen activity in lead–bismuth may be lower than necessary to form magnetite but enough to form oxide of less noble elements like chromium. The low oxygen activity is supported by the solution process observed in B and C specimens, and is questioned by the growth of oxide in type A specimens. On the other hand, a high iron concentration was measured in a eutectic sample taken out during the loop operation. This high iron concentration can hinder iron diffusion and prevent magnetite formation.

At present we have no plausible explanation for the observed behaviour in similar specimens tested during the same period at different loop operation moments. However, the growth of oxide layer in A specimens simultaneously with the solution in B and C specimens points out that oxide layer growth needs lower oxygen activity than oxide layer formation.

5. Conclusions

The results obtained in this experimental work point out that oxide layer protection of martensitic steels in lead–bismuth under temperature gradient is possible in determined conditions. Higher oxygen activity seems to be necessary for oxide formation than for oxide layer growth. A double oxide layer is formed on martensitic steel in liquid lead–bismuth.

The oxide layer is formed by a magnetite outer layer and a spinel $Fe(Fe_{2-x})Cr_xO_4$ inner layer, very rich in chromium. Th spinel is non-permeable to lead–bismuth and constitutes a barrier between base material and liquid metal.

It is possible to operate a natural convection loop for long times up to 3000 h without plugs appearance. However, impurities in the melt, coming from the structural material dissolution, interfere with the oxide layer formation on the samples tested, and lead to a difficult interpretation of the obtained results.

References

[1] J.J. Park et al., Nucl. Eng. Des. 196 (2000) 315.
[2] I.V. Gorynin, G.P. Karzov, V.G. Markov, V.A. Yakovlev, Met. Sci. Heat Treat. 41 (9–10) (1999).
[3] G.M. Tolson, A. Taboada, A study of lead and lead-salt corrosion in thermal-convection loops, ORNL-TM-1437, April 1966.
[4] K.D. Childs et al., Handbook of Auger Electron Spectroscopy, Physical Electronics, Eden Prairie, MN, 1995.
[5] AES PC-ACESS, Software Manual, Physical Electronics, Eden Prairie, MN, 1998.
[6] B.F. Gromov, Y.I. Orlov, P.N. Martynov, V.A. Gulersky, The problems of technology of the heavy liquid metals coolants (Lead–Bismuth, Lead), Heavy Liquid Metals Coolant in Nuclear Techology, HLMC 98, Obninsk 1998.
[7] J.R.Weeks, C.J. Klamut, Liquid Metal Corrosion Mechanisms, in: Proceedings of the Conference on Corrosion of Reactor Materials, IAEA, Vienna 1962.
[8] G.C. Woods, Corros. Sci. 2 (1961) 173.
[9] V.M. Fedirko, O.I. Eliseeva, V.L. Kalyandruk, V.A. Lopushans'kyi, Mater. Sci. 33 (3) (1977).
[10] V.M. Fedirko, O.I. Eliseeva, V.L. Kalyandruk, V.A. Lopushans'kyi, Mater. Sci. 33 (2) (1977).
[11] G. Benamati, P. Buttol, V. Imbeni, C. Martini, G. Palombarini, J. Nucl. Mater. 279 (2000) 308.
[12] G. Müller, G. Schumacher, F. Zimmermann, J. Nucl. Mater. 278 (2000) 85.
[13] J. Robertson, Corros. Sci. 2 (4) (1991) 443.